

Air-Aided Communication Between Ground Assets in a Poisson Forest

Juan David Pabon, Shaikha Alkandari, Matthew C. Valenti, and Xi Yu
West Virginia University, Morgantown, WV, USA.

Abstract—Ground assets deployed in a cluttered environment with randomized obstacles (*e.g.*, a forest) may experience line of sight (LoS) obstruction due to those obstacles. Air assets can be deployed in the vicinity to aid the communication by establishing two-hop paths between the ground assets. Obstacles that are taller than a position-dependent critical height may still obstruct the LoS between a ground asset and an air asset. In this paper, we provide an analytical framework for computing the probability of obtaining a LoS path in a Poisson forest. Given the locations and heights of a ground asset and an air asset, we establish the critical height, which is a function of distance. To account for this dependence on distance, the blocking is modeled as an inhomogeneous Poisson point process, and the LoS probability is its void probability. Examples and closed-form expressions are provided for two obstruction height distributions: uniform and truncated Gaussian. The examples are validated through simulation. Additionally, the end-to-end throughput is determined and shown to be a metric that balances communication distance with the impact of LoS blockage. Throughput is used to determine the range at which it is better to relay communications through the air asset, and, when the air asset is deployed, its optimal height.

I. INTRODUCTION

Many military communication scenarios involve the deployment of heterogeneous teams of mobile assets that execute joint tasks in challenging environments, such as forests, where randomized obstacles are located. Often these tasks are autonomous and the assets may be robotic. Potential application scenarios range from exploring and monitoring sensitive areas to search and rescue [1]–[6]. In such scenarios, different mobile assets in the same team need to coordinate with each other and perform tasks jointly. Information sharing is an essential piece to the coordination of the team members [7] and can be realized via data streaming from one asset to another.

Computer-aided localization and mapping [8], [9] relying on cameras and laser devices have been developed to realize high-quality environment modeling in forests. Camera or laser enabled modeling and monitoring techniques usually require the mobile asset to continuously see the objects (*e.g.*, its teammates) being monitored. Cutting-edge communication technologies use short wavelengths, such as in millimeter-wave (mmwave) or even terahertz (THz) bands, to enhance the transmission speed, but the penetration capability is limited and usually requires a line of sight (LoS) to close a link. Motivated by these examples and others like it, it is clear that maintaining a line of sight (LoS) is preferred between these kinds of mobile assets.

Various existing works related to environments with obstacles focus on planning for the best routes for mobile assets or the optimal locations for stationary assets to avoid the connections between certain pairs of assets being blocked by

the obstacles [10]. Such methods rely on perfect knowledge of the locations of the obstacles. In reality, this type of knowledge may be expensive to acquire, especially for large-scale areas.

Locations of obstacles randomly distributed in a cluttered 2-D environment can be seen as generated via a Poisson point process (PPP). Such a model is usually referred to as a *Poisson Forest*. Extensive work has been done related to navigating mobile assets in such forests [11]–[13]. Probabilities of having LoS of a minimum length in such a 2-D environment are also computed [11] and related to the density of the PPP.

Because a given team may deploy heterogeneous mobile assets located at different altitudes (*e.g.* both ground assets and air assets), it is essential to consider the 3-D nature of the environment. Not only the thickness and the locations of the obstacles need to be considered, but also the *heights* of the obstacles are important. References [14]–[16] address the height distribution of obstacles in an urban environment with semi-randomly distributed obstacles. References [17], [18] model urban areas with obstacles of random heights using the Manhattan Point Line Process to address the grid-like patterns of the obstacles' locations. This series of work points out that only obstacles taller than a *critical height* can block the LoS between a ground asset and an air asset. The critical height is a location-dependent function that depends on the ground and the air assets' locations as well as the height that the air asset is flying at. Any obstacle that is taller than the critical height evaluated at that obstacle's location will block the LoS.

In this paper, we study the 3-D LoS between heterogeneous assets in a Poisson forest. We calculate the critical height, *i.e.*, the height above which an obstacle is able to block the LoS, at any given location between a pair of assets. The distribution of the obstacles above the critical height is then modeled as an *inhomogeneous* PPP. By finding the void probability of the inhomogeneous PPP, we are able to determine the probability of obtaining LoS. Examples and expressions that are in closed form (up to known standard functions) are provided for two obstruction height distributions: uniform and truncated Gaussian. The examples are validated through simulation. Additionally, we establish *throughput* as a metric that balances communication distance with the impact of LoS blockage. Throughput is used to determine the range at which it is better to relay communications through the air asset, and, when the air asset is deployed, its optimal height.

The paper is organized as follows. Sec. II formulates the problem. Sec. III analyzes the probability of obtaining LoS between a pair of assets. Sec. IV discusses the throughput of the communication among assets. Sec. V provides numerical results derived from our methods as well as simulation vali-

dations. Sec. VI concludes the paper.

II. PROBLEM FORMULATION

Consider a pair of ground assets, each equipped with a communication device (*e.g.*, an antenna, a camera, etc.) at a height of h_g , deployed in a planar task space (*e.g.*, a forest) with stochastically distributed obstacles (*e.g.*, trees) of a non-trivial thickness. The locations of the obstacles are generated by a two-dimensional Poisson Point Process with a fixed density λ_f . Let N be the number of obstacles in a task space of area A_f and λ_f be the intensity of the PPP representing the expected number of obstacles per unit area. From the basic properties of a PPP

$$\mathbb{P}\{N = n\} = \frac{(\lambda_f A_f)^n}{n!} e^{-\lambda_f A_f},$$

Such a task space is referred to as a *Poisson forest*.

The height of any single obstacle in the Poisson forest is represented by a non-negative random variable H_t . The distribution of H_t may vary. We denote the cumulative distribution function (cdf) of H_t as $F_H(h)$. Evaluating $F_H(h)$ at a given height h_0 gives the probability that a given obstacle has a height that is less than or equal to h_0 .

The analysis in this paper does not require that H_t assumes any particular distribution. In fact, the height distribution of trees in a forest varies [19]–[21]. Bell-shaped distributions [20] and positive-skewed distributions [19] can both be found. To provide specific realistic cases, without any loss of generality, we consider a single-sided truncated Gaussian distribution and a uniform distribution as examples to illustrate our methods. Both examples are constructed such that the heights are non-negative.

The truncated Gaussian uses a Gaussian random variable with mean μ and standard deviation σ as its parent distribution, and is truncated to the range $h \geq 0$. The cdf of this variable is

$$F_H(h) = \frac{Q\left(\frac{\mu - h}{\sigma}\right) - Q\left(\frac{\mu}{\sigma}\right)}{1 - Q\left(\frac{\mu}{\sigma}\right)}, \quad (1)$$

for $h \geq 0$, and zero elsewhere, where $Q(\cdot)$ is the Q-function.

For the uniform distribution, the cdf is

$$F_H(h) = \begin{cases} 0 & \text{for } h < 0 \\ \frac{h}{h_{\max}} & \text{for } 0 \leq h \leq h_{\max} \\ 1 & \text{for } h > h_{\max} \end{cases}, \quad (2)$$

where h_{\max} is the maximum height of the obstruction.

Now consider the one-dimensional space between the two ground assets. Let the locations of the two ground assets be 0 and x_g on this 1-D coordinate system. Any obstacle with a height above h_g located along the interval $(0, x_g)$ would potentially block the unobstructed view of one ground asset on the other. If there is no such obstacle, we consider there is a *line of sight* (LoS) between the two ground assets.

In the above-mentioned Poisson forest, the expected number of obstacles located exactly along the one-dimensional space $(0, x_g)$ should be zero since the Lebesgue Measure of a

straight line in a two-dimensional space is always zero. However, when the obstacles' thicknesses are non-trivial, obstacles located in a finite area with a non-trivial width around the line $(0, x_g)$ may also block the LoS between the two ground assets. Therefore we consider the distribution of potential obstacles along a straight line in this Poisson forest to be characterized by a 1-D Poisson Process with a fixed density λ_0 capturing the expected number of obstacles located along a straight line of unit length. λ_0 is determined by $\lambda_0 = E(w)\lambda_f$, where $E(w)$ is the average thickness of obstacles.

Now consider the case that an air asset at an altitude or height of h_a is available to aid in the communication, for instance, by receiving the signal transmitted to it by the first ground asset and relaying it to the second ground asset. In this paper, we limit the horizontal location of the air asset to be along the straight line $(0, x_g)$ that connects the two ground assets. If we define x_a to be the horizontal location of the air asset, then $0 \leq x_a \leq x_g$.

In the following sections, we calculate the probabilities of obtaining a LoS in ground-ground, ground-air, and ground-air-ground (*i.e.*, air-aided) connections, and calculate the throughput in all these scenarios. We furthermore find the throughput for these cases. Our calculations provide conditions under which air assets should be deployed to aid the connections between ground assets and provide insight into the optimal height of the air asset when one is deployed.

III. PROBABILITY OF OBTAINING LOS

In this section, we provide methods for calculating the probabilities of obtaining a LoS (*i.e.*, the *LoS probability*), between a pair of ground assets as well as between one ground asset and one air asset.

A. Critical height

In the Poisson forest introduced in the previous section, only obstacles that are above a certain height will block the view between two assets. If the two assets are both on the ground and have their communication devices at the same height h_g , only obstacles with heights greater than h_g may block the LoS. In this case, we say h_g is the critical height h_c of the obstacles.

When considering the LoS between a ground asset of height h_g and an air asset of height h_a , the critical height is determined by the straight line connecting the communication devices of the ground asset and the air asset which is located at x_a , as shown in Fig. 1. Given both assets are fixed, the critical height is a function of the location $x \in [0, x_a]$ along the horizontal coordinate. As can be seen in Fig. 1, the critical height is low close to the ground asset, where even short obstructions can block the LoS, but is high further away from the ground asset, where only the tallest obstructions can block the LoS. The critical-height function is

$$h_c(x) = \frac{h_a - h_g}{x_a}x + h_g. \quad (3)$$

Notice that $h_c(x)$ increases linearly with x increasing from 0 to x_a .

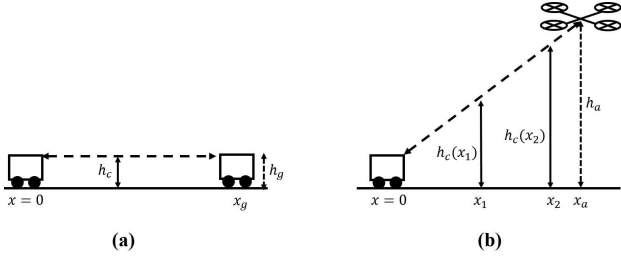


Fig. 1: (a) shows the critical height of obstacles between a pair of ground assets. (b) shows the critical height determined by the straight line between a ground asset and an air asset.

B. Inhomogeneous Poisson Point Process

As introduced in Sec. II, the location of obstacles are generated by a homogeneous PPP with density λ_0 . Consider the case that the critical height h_c is a constant, such as with the direct ground-ground link. Since not all the obstacles are tall enough to block the LoS between assets, we must retain only those obstacles whose heights are higher than h_c . For any random obstacle, the probability that it has a height h_o greater than h_c can be calculated by

$$\mathbb{P}\{h_o > h_c\} = 1 - F_H(h_c).$$

Therefore, the distribution of obstacles with heights greater than h_c in this Poisson forest can be modeled as a Poisson process with its density λ_c defined as

$$\lambda_c = \lambda_0 \mathbb{P}\{h_o > h_c\} = \lambda_0 [1 - F_H(h_c)]. \quad (4)$$

When h_c is location-dependent as in (3), this model becomes an inhomogeneous Poisson process with a location-dependent density $\lambda(x)$ defined as

$$\lambda(x) = \lambda_0 [1 - F_H(h_c(x))]. \quad (5)$$

For a given $F_H(\cdot)$ (e.g (1) or (2)), the cumulative probability towards a given h increases with h . Therefore, $\lambda(x)$ decreases monotonically when h increases. That is to say, in a given Poisson forest, with a greater critical height, the probability of having obstacles taller than this critical height is lower.

C. LoS between a pair of ground assets

As discussed in Sec. III-A, only obstacles with heights above h_g will block the direct view between a pair of ground assets. Therefore we set the critical height $h_c = h_g$. Since h_c is constant, the blockages are described by the homogeneous PPP given by (4). Therefore, the probability of obtaining a LoS between a pair of ground assets that are located at 0 and x_g is found from the void probability of the homogeneous PPP of density $\lambda_c = \lambda_0 [1 - F_H(h_c)]$ over an interval of length x_g . This probability is

$$\mathbb{P}_{LoS}^{gg}(x) = e^{-\lambda_0 [1 - F_H(h_g)] x_g}, \quad (6)$$

D. LoS between a ground asset and an air asset

The distribution of obstacles along the straight line from the ground asset ($x = 0$) to the air asset ($x = x_a$) can be modeled as a Poisson process with a density of λ_0 . The critical height, above which an obstacle may block the LoS between the two assets, varies depending on the location of the obstacle. Therefore, the distribution of the obstacles that are tall enough to disrupt the unobstructed view fits an inhomogeneous Poisson process with a location-dependent density defined as in (5).

The probability of having no obstacle blocking the LoS between a ground asset at 0 and an air asset at x_a is found from the void probability of the inhomogeneous PPP, which is found as follows

$$\mathbb{P}_{LoS}^{ga}(x) = \exp\left(-\int_0^{x_a} \lambda(x) dx\right). \quad (7)$$

Finding a solution to (7) depends on the difficulty of performing the integration, which depends on the nature of $F_H(h)$. In some cases, such as the two examples provided below, closed-form solutions can be found, at least up to being expressed in terms of well-known expressions. Alternatively, when closed-form solutions cannot be readily obtained, (7) can be solved numerically, for instance, by using numerical integration.

For the two different heights distributions mentioned in Sec.II, we can find the analytical solutions of (7). Sec. III-E and Sec.III-F show the analytical solutions for the truncated Gaussian and uniform distributions.

E. P_{LoS}^{ga} for truncated Gaussian distribution

For the truncated Gaussian distribution, the density of the inhomogeneous PPP is given by (5), where $F_H(\cdot)$ is given by (1) and $h_c(\cdot)$ is given in (3). The resulting density is

$$\lambda(x) = \lambda_0 \left(\frac{\Phi\left(\frac{\mu - h_c(x)}{\sigma}\right)}{\Phi\left(\frac{\mu}{\sigma}\right)} \right),$$

where

$$\Phi(z) = 1 - Q(z) = \frac{1}{2} \left(1 + \operatorname{erf}\left(\frac{z}{\sqrt{2}}\right) \right) \quad (8)$$

is the cdf of the standard normal distribution.

The integral in (7) is

$$\int_0^{x_a} \lambda(x) dx = \frac{\lambda_0}{\Phi\left(\frac{\mu}{\sigma}\right)} \int_0^{x_a} \Phi\left(\frac{\mu - h_c(x)}{\sigma}\right) dx.$$

From (8), this can be rewritten as

$$\begin{aligned} \int_0^{x_a} \lambda(x) dx &= c \int_0^{x_a} (1 + \operatorname{erf}(a - bx)) dx \\ &= c \left(x_a + \int_0^{x_a} \operatorname{erf}(a - bx) dx \right) \end{aligned} \quad (9)$$

where $a = (\mu - h_g)/(\sqrt{2}\sigma)$, $b = (h_a - h_g)(\sqrt{2}\sigma x_a)$ and $c = \lambda_0 / (2\Phi(\mu/\sigma))$.

The integral on the second line of (9) can be found from mathematical handbooks (e.g. [22]) to be

$$\frac{e^{-a^2} + \sqrt{\pi} [(bx_a - a)\text{erf}(a - bx_a) + \text{aerf}(a)] - e^{-(a-bx_a)^2}}{\sqrt{\pi}b}. \quad (10)$$

The LoS probability is then found by substituting (9) into (7) with the integral in the second line of (9) set to (10).

F. Analytical solution of \mathbb{P}_{LoS}^{ga} for uniform distribution

For the uniform distribution, the density of the inhomogeneous PPP is given by (5), where $F_H(\cdot)$ is given by (2) and $h_c(\cdot)$ is again given in (3). Evaluating $F_H(h_c(x))$ we obtain

$$F_H(h_c(x)) = \begin{cases} 0 & \text{for } x \leq x' \\ \left(\frac{h_a - h_g}{x_a h_{\max}}\right)x + \frac{h_g}{h_{\max}} & \text{for } x' < x \leq x_c \\ 1 & \text{for } x > x_c \end{cases} \quad (11)$$

where $x' = -h_g x_a / (h_a - h_g)$ and x_c is the critical distance at which any obstacle located at a distance $x > x_c$ cannot block the LoS since $h_c(x) > h_{\max}$. This distance is given by

$$x_c = \left(\frac{h_{\max} - h_g}{h_a - h_g}\right)x_a$$

since x' is negative it is inconsequential, since the integral of (7) does not cover negative x . The density of the inhomogeneous PPP is found by substituting (11) into (5) resulting in

$$\lambda(x) = \begin{cases} \lambda_0 \left[1 - \left(\frac{h_a - h_g}{x_a h_{\max}}\right)x - \frac{h_g}{h_{\max}}\right] & \text{for } 0 < x \leq x_c \\ 0 & \text{for } x > x_c. \end{cases} \quad (12)$$

From (7), $\mathbb{P}_{LoS}^{ga}(x_a)$ requires that $\lambda(x)$ be integrated from 0 to x_a . If $x_a \leq x_c$, then

$$\int_0^{x_a} \lambda(x) dx = \int_0^{x_a} \lambda_0 \left[1 - \left(\frac{h_a - h_g}{x_a h_{\max}}\right)x - \frac{h_g}{h_{\max}}\right] dx. \quad (13)$$

When $x_a > x_c$, $\lambda(x) = 0$ for $x > x_c$ and thus the integral from x_c to x_a is zero. It follows then that the integral will take the same form as in (13) but the upper limit can be tightened to x_c since the integral beyond that point is zero.

Rather than expressing the integral separately for the two cases of $x_a \leq x_c$ and $x_a > x_c$, we can express them as the following single expression

$$\int_0^{x_a} \lambda(x) dx = \lambda_0 \int_0^{\min(x_a, x_c)} \left[1 - \left(\frac{h_a - h_g}{x_a h_{\max}}\right)x - \frac{h_g}{h_{\max}}\right] dx.$$

defining λ_u as the solution of the previous integral we have

$$\lambda_u = \lambda_0 \min(x_a, x_c) \left[1 - \frac{h_g}{h_{\max}} - \left(\frac{h_a - h_g}{2x_a h_{\max}}\right) \min(x_a, x_c)\right].$$

Then, using λ_u we get that the probability of obtaining LoS for ground-air communication \mathbb{P}_{LoS}^{gh} at $x = x_a$ is given by

$$\mathbb{P}_{LoS}^{ga}(x_a) = e^{-\lambda_u}.$$

IV. CALCULATING THE THROUGHPUT

While the LoS probability is useful for predicting the existence of a LoS between two assets, it does not characterize the *quality* of the link, which is also affected by the transmission distance of each link. For instance, if one wants to determine the height of an air asset that maximizes *only* the end-to-end LoS probability with a ground asset, the solution would be to place the air asset at an infinite height so that the critical heights at any location between the two assets are infinite (*i.e.*, no obstacle is able to block the unobstructed view between them). Such solution is neither practical nor efficient in reality due to the significant signal loss caused by the infinite transmission distance.

An appropriate metric that captures the loss of signal power at distance is the expected *throughput*, which we here define to be the maximum achievable data rate when accounting for the possibility of blockage. This definition makes sense considering a mixed team of ground and air assets navigating through the forest and maintaining communication. The probability of LoS between any pair of assets yields an expected communication time, which contributes to an expected throughput that can be achieved. For a single hop, the expected throughput is

$$T = \mathbb{P}_{LoS} C, \quad (14)$$

where C is the *capacity* of the link, and the multiplication by \mathbb{P}_{LoS} accounts for the expectation being with respect to LoS. Here, we set C as the Shannon Capacity, which is the maximum achievable rate of an unblocked link

$$C = B \log_2(1 + \text{SNR}), \quad (15)$$

where B is the signal bandwidth, and the signal-to-noise ratio, when expressed in dB, is

$$\text{SNR}^{\text{dB}} = \text{SNR}_0^{\text{dB}} - 10\alpha \log_{10}\left(\frac{d}{d_0}\right), \quad (16)$$

where α is the path-loss exponent, d_0 is a reference distance typically set to 1 meter, and SNR_0^{dB} is the SNR when the receiver is placed at distance d_0 assuming free-space propagation up to that distance. The value of SNR_0^{dB} can be measured, or it can be calculated from the transmit power, carrier frequency, bandwidth, receiver's noise figure, and antenna gains.

For a direct ground-ground transmission, the expected throughput is computed from (14) with d in (16) set to x_g . For a two-hop ground-air-ground transmission, it depends on the LoS probabilities of both hops. Let $\mathbb{P}_{LoS}^{\text{ga}}$ and $\mathbb{P}_{LoS}^{\text{ag}}$ be the LoS probabilities of the ground-to-air and air-to-ground links, respectively, and similarly define C_{ga} and C_{ag} as the two capacities, the expected throughput for the ground-air-ground communication is

$$T = \frac{1}{2} \mathbb{P}_{LoS}^{\text{ga}} \mathbb{P}_{LoS}^{\text{ag}} \min(C_{\text{ga}}, C_{\text{ag}}), \quad (17)$$

where the multiplication by 1/2 accounts for the time-division duplexing (TDD) operation at the air asset (*i.e.*, the air asset spends half its time receiving from the first ground asset and half its time transmitting to the second ground asset). Alternatively, frequency-division duplexing (FDD) can be used, but in

that case, the per-link capacities should be scaled accordingly since only half of the band could be used for each hop. Each capacity is found from (15) with the distance in (16) set as the Euclidean distance between the air antenna and the corresponding ground antenna, where each distance is the hypotenuse of a right triangle formed with one leg being the horizontal distance, either x_a for the ground-air link or $x_g - x_a$ for the air-ground link, and the other leg being the difference in antenna heights, $h_a - h_g$. Notice that the ground-air-ground throughput is determined by the minimum capacity of the two hops, which motivates us to consider deploying the aiding air asset always above the midpoint of the two ground assets.

V. SIMULATION-VALIDATED NUMERICAL RESULTS

In this section, we present numerical results generated by our methods. The key part of these methods is the calculation of the probability of obtaining a LoS between different types of assets. We consider a Poisson forest where the locations of the obstacles along a straight line are generated via a Poisson point process with $\lambda_0 = 0.02$. The distributions of the obstacle height H_t were chosen to be a truncated Gaussian distribution with cdf $F_H(h)$ defined as in (1) with $\mu = 19$ m and $\sigma = 10$ m and a uniform distribution with cdf $F_H(h)$ defined as in (2) with $h_{\max} = 29$ m. The choice of the parameters is consistent with the parameters chosen in [18].

To validate the numerical results, we performed Monte Carlo simulations involving the repeated drawing of Poisson forests. Let ℓ be the interval of a simulated Poisson forest, where $\ell = x_g$ for a ground-ground link or $\ell = x_a$ for a ground-air link. Drawing a Poisson forest involves first determining the random number N of obstructions in the interval, which is done by drawing N from a Poisson distribution of mean $\lambda_0 \ell$. Next, each of the N obstructions is placed uniformly over the interval. Then, each obstruction's height is determined by randomly drawing its H from the corresponding distribution. Once the forest was constructed, it was determined whether or not the LoS path was blocked by checking to see if any of the obstructions were above the critical height at that location. This process was repeated for 500 thousand trials for each data point reported.

Fig. 2 shows the probability of obtaining LoS between a ground asset and an air asset, $\mathbb{P}_{LoS}^{ga}(x)$, with the horizontal distance x_a . In this figure, only the truncated Gaussian distribution is considered, as results for the uniform distribution are similar. The air asset flies at different fixed heights of 50, 100, and 200 meters. The ground asset has a communication device fixed at the height of $h_g = 2$ meters. The results in Fig. 2 show that $\mathbb{P}_{LoS}^{ga}(x)$ decreases as x_a increases. The reason is straightforward. A longer distance between the two assets simply allows a greater probability of having obstacles in between. Meanwhile, $\mathbb{P}_{LoS}^{ga}(x)$ increases as h_a increases. This is because the critical height will increase with a greater h_a (as in (3)). A greater critical height rejects more obstacles from potentially blocking the LoS between the two assets. Therefore flying the air asset at a higher altitude generally increases the probability of obtaining LoS.

Increasing the height h_g of the communication devices carried by the ground asset will improve the probability of

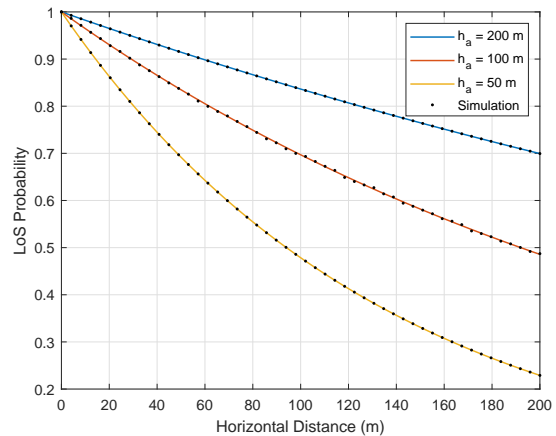


Fig. 2: Probability of obtaining LoS from a ground asset located at 0 and to an air asset located at x_a for a truncated Gaussian height distribution and $h_g = 2$ m. Solid lines show the numerical results calculated using our closed-form expressions, while the dots show results generated by Monte Carlo simulation.

obtaining LoS as well. Generally, increasing the height of the ground assets' communication devices is a more expensive and less efficient way to enhance the probability of LoS as compared with increasing the height of the air asset. For practical purposes, a big increase of h_g is not preferable, but a small increase may result in an acceptable increase of the $\mathbb{P}_{LoS}^{ga}(x)$ for shorter distances.

We then compare the end-to-end LoS probability \mathbb{P}_{LoS} of direct ground-ground communication with air-aided ground-air-ground communication. When making this comparison, the air asset is always deployed above the midpoint of the two ground assets; *i.e.*, $x_a = x_g/2$. In this scenario, the probability to obtain LoS from the air asset to both ground assets synchronously is the square of \mathbb{P}_{LoS}^{ga} . We assume that the air asset is flying at a height of $h_a = 100$ m, while all ground assets have their communication devices fixed at a height of $h_g = 2$ m. Both the truncated Gaussian and the uniform height distributions are considered. Fig. 3 shows the results of this comparison. For direct ground-ground communication, the probability of obtaining LoS decreases much faster as a function of distance than in the case of air-aided ground-air-ground communication. For the truncated Gaussian distribution, when $\mu = 19$ m and $\sigma = 10$ m, (1) suggests that most of the obstacles will be taller than 2 m. Thus, almost all obstacles can block the unobstructed view between a pair of ground assets, severely decreasing the probability of obtaining the LoS. For the uniform distribution, according to (2), there is a probability greater than 0.92 that the heights of the obstacles are taller than h_g . This causes a fast decrease in the \mathbb{P}_{LoS} for the ground-ground communication, which is similar to what is observed for the truncated Gaussian distribution.

When $x_a = 60$ m, (*i.e.* $x_g = 120$ m), the probability of obtaining LoS between ground assets using direct ground-ground communication is approximately 0.1 for both the truncated Gaussian and the uniform distributions. However,

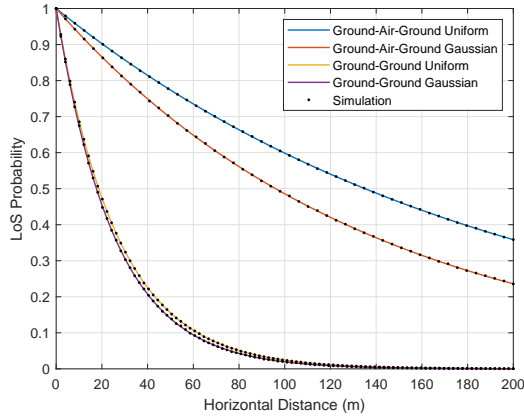


Fig. 3: Probabilities of obtaining the LoS for ground-air-ground and ground-ground communication for $h_a = 100$ m and $h_g = 2$ m. Solid lines show the numerical results calculated using our closed-form expressions, while the dots show results generated by Monte Carlo simulation.

when an air asset is used, the probability that it obtains a LoS with both ground assets is approximately 6.5 and 7.3 times greater than the probability of the two ground assets obtaining LoS over a direct link considering the truncated Gaussian and uniform distributions, respectively. Fig. 3 shows that the choice of distribution does not have a significant impact on the probability of obtaining the LoS between ground assets using the direct link, since the communication devices of the ground assets are fixed at a relatively low height and therefore the LoS would be easily blocked by most obstacles. On the other hand, when an air asset is used, the height distribution has a bigger impact on the LoS probability since the differences of the distributions become more pronounced.

In addition, we computed the throughput performance for the same scenarios previously discussed. The additional parameters required to compute the throughput are a reference SNR of $\text{SNR}_0^{\text{dB}} = 51.98$ dB at a reference distance of $d_0 = 1$ meter, a path-loss coefficient of $\alpha = 2.3$, and a bandwidth of $B = 20$ MHz. This path-loss coefficient corresponds to the one reported in [23] for the measured LoS pathloss at 38 GHz. The reference SNR is computed for a transmit power of 0 dBm, a receiver noise figure of 9 dB, and antenna gains of 12.1 dBi for both the transmit and receive antennas, which are the gains reported for a compact 6-element array operating at 38 GHz in [24]. We consider the same obstacle models as before, with $\lambda = 0.02$ and height distributions that are either a truncated Gaussian (with $\mu = 19$ and $\sigma = 10$) or a uniform (with $h_{max} = 29$). The ground asset's antenna height is set to $h_g = 2$ m.

Fig. 4 shows throughput as a function of the height of the air asset, h_a , for several different distances between ground assets, x_g . The air asset is located at the midpoint between the two ground assets, *i.e.* $x_a = x_g/2$, and this figure shows results for just the truncated Gaussian height distribution (results for the uniform distribution are similar). As expected, the throughput is higher when the ground assets are closer to each

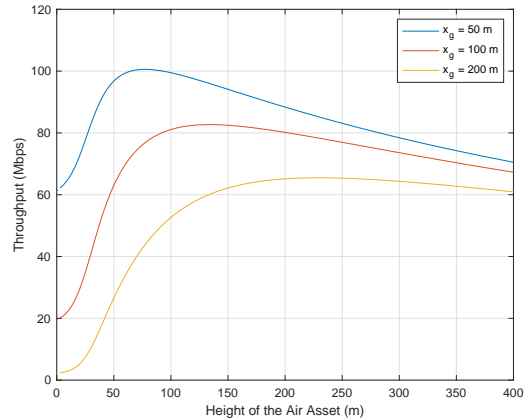


Fig. 4: Throughput of ground-air-ground communication as a function of the height h_a of the air asset for horizontal distances $x_g = \{50, 100, 200\}$ m considering a Gaussian truncated distribution and $h_g = 2$ m.

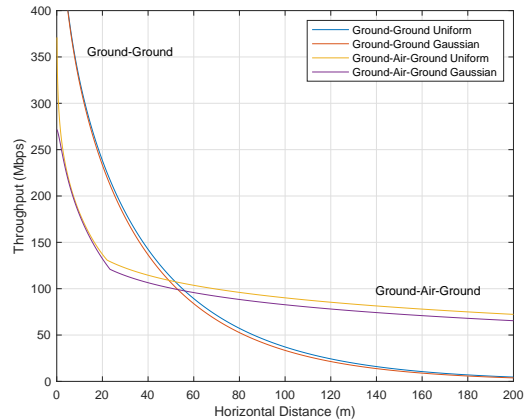


Fig. 5: Throughput as a function of horizontal distance x_g for both truncated Gaussian and uniform height distributions. Results are shown for direct ground-ground communication as well as for relayed ground-air-ground communication. In the case of ground-air-ground communication, the throughput is optimized with respect to the height h_a of the air asset.

other. However, for each curve, a peak value can be observed. Lowering the altitude of the air asset below this peak makes it prone to blocking, but raising it above the peak value causes a loss in signal power which translates to a loss of capacity. The peak value balances the assets' capability of obtaining LoS and the signal power, which is a key tradeoff as both contribute to the throughput. For x_g equal to 50 m, 100 m, and 200 m, the peak values are 100.6 Mbps, 82.7 Mbps, and 65.5 Mbps, respectively, and these peaks occur at h_a of 77 m, 134 m, and 230 m, respectively.

Fig. 5 shows throughput as a function of the horizontal distance x_g between the ground assets. The figure shows results for both truncated Gaussian and uniform height distributions and for both direct ground-ground communication and relayed ground-air-ground communication. For ground-

air-ground communication, the throughput is optimized at each distance by maximizing its value over the height of the air asset h_a . For direct ground-ground communication, no such optimization is possible. The plot shows that, for sufficiently far distances, the throughput of the ground-air-ground communication is higher than that of the direct ground-ground communication. However, for shorter distances, ground-ground communication has a higher throughput. When the height distribution is a truncated Gaussian, this crossover occurs at a distance of $x_g = 52.9$ m, where the throughput for both direct ground-ground and relayed ground-air-ground communications is 99 Mbps. The reason that direct ground-ground communications performs better at ranges closer than this crossover distance is primarily due to the need for the air asset to duplex the signal received from the first ground asset and transmitted to the second ground asset. The direct link does not need to duplex. However, at longer distances, maintaining a direct link between the two ground assets suffers from a lower probability of obtaining a LoS and a weaker signal power due to the long single transmission path.

VI. CONCLUSIONS AND FUTURE WORK

In this paper, we studied issues related to deploying an air asset in a Poisson forest to aid the connection between a pair of ground assets. The key contribution is a framework for calculating the LoS probability and the throughput. This framework depends on carefully considering the location-dependent critical height, which is the minimum height required for an obstruction at that location to block the LoS. Because the critical height is distance dependent, the distribution of obstacles that are above the critical height is an inhomogeneous Poisson point process even if the location of the obstructions themselves is a homogeneous PPP. Closed-form results are provided for two height distributions: truncated Gaussian and uniform. Simulation results validate the theoretical expressions.

The theory enables the solution to two particular problems. First, it allows the determination of a crossover distance, below which it is better for the ground assets to communicate directly, and above which air-assistance is desirable. Second, it allows for the determination of the optimal height of the air asset when one is used. The key to solving these problems is to use throughput as the performance metric, as throughput can properly balance the tradeoff wherein higher altitudes increase the LoS probability but reduce signal power.

This work is a gateway to optimally deploying a heterogeneous team of mobile air assets and ground assets in a dense forest. Future works include planning for the optimal deployment of the air assets given a known or unknown layout of the ground assets, and planning the optimal trajectories for the joint team to navigate through the task space while staying connected and coordinating on task delivery.

REFERENCES

- [1] J. Langelaan and S. Rock, "Towards autonomous uav flight in forests," in *AIAA Guidance, Navigation, and Control Conference and Exhibit*, 2005, p. 5870.
- [2] X. Zheng, S. Koenig, D. Kempe, and S. Jain, "Multirobot forest coverage for weighted and unweighted terrain," *IEEE Transactions on Robotics*, vol. 26, no. 6, pp. 1018–1031, 2010.
- [3] K. Harikumar, J. Senthilnath, and S. Sundaram, "Multi-uav oxyrrhis marina-inspired search and dynamic formation control for forest fire-fighting," *IEEE Transactions on Automation Science and Engineering*, vol. 16, no. 2, pp. 863–873, 2018.
- [4] M. S. Couceiro, D. Portugal, J. F. Ferreira, and R. P. Rocha, "Semfire: Towards a new generation of forestry maintenance multi-robot systems," in *2019 IEEE/SICE International Symposium on System Integration (SII)*. IEEE, 2019, pp. 270–276.
- [5] Y. Tian, K. Liu, K. Ok, L. Tran, D. Allen, N. Roy, and J. P. How, "Search and rescue under the forest canopy using multiple uavs," *The International Journal of Robotics Research*, vol. 39, no. 10-11, pp. 1201–1221, 2020.
- [6] L. F. Oliveira, A. P. Moreira, and M. F. Silva, "Advances in forest robotics: A state-of-the-art survey," *Robotics*, vol. 10, no. 2, p. 53, 2021.
- [7] R. Doriya, S. Mishra, and S. Gupta, "A brief survey and analysis of multi-robot communication and coordination," in *International Conference on Computing, Communication & Automation*. IEEE, 2015, pp. 1014–1021.
- [8] M. F. Mysorewala, D. O. Popa, and F. L. Lewis, "Multi-scale adaptive sampling with mobile agents for mapping of forest fires," *Journal of Intelligent and Robotic Systems*, vol. 54, no. 4, pp. 535–565, 2009.
- [9] B. Benjamin, G. Erinc, and S. Carpin, "Real-time wifi localization of heterogeneous robot teams using an online random forest," *Autonomous robots*, vol. 39, no. 2, pp. 155–167, 2015.
- [10] A. Gasparetto, P. Boscaroli, A. Lanzutti, and R. Vidoni, "Path planning and trajectory planning algorithms: A general overview," *Motion and operation planning of robotic systems*, pp. 3–27, 2015.
- [11] S. Karaman and E. Frazzoli, "High-speed flight in an ergodic forest," in *2012 IEEE International Conference on Robotics and Automation*. IEEE, 2012, pp. 2899–2906.
- [12] —, "High-speed motion with limited sensing range in a poisson forest," in *2012 IEEE 51st IEEE Conference on Decision and Control (CDC)*. IEEE, 2012, pp. 3735–3740.
- [13] B. Martinez R and G. A. Pereira, "Fast path computation using lattices in the sensor-space for forest navigation," in *2021 IEEE International Conference on Robotics and Automation (ICRA)*. IEEE, 2021, pp. 1117–1123.
- [14] E. Hriba, M. C. Valenti, K. Venugopal, and R. W. Heath, "Accurately accounting for random blockage in device-to-device mmwave networks," in *GLOBECOM 2017-2017 IEEE Global Communications Conference*. IEEE, 2017, pp. 1–6.
- [15] E. Hriba and M. C. Valenti, "The impact of correlated blocking on millimeter-wave personal networks," in *MILCOM 2018-2018 IEEE Military Communications Conference (MILCOM)*. IEEE, 2018, pp. 1–6.
- [16] E. Hriba, M. C. Valenti, and R. W. Heath, "Optimization of a millimeter-wave uav-to-ground network in urban deployments," in *MILCOM 2021-2021 IEEE Military Communications Conference (MILCOM)*. IEEE, 2021, pp. 861–867.
- [17] F. Baccelli and X. Zhang, "A correlated shadowing model for urban wireless networks," in *2015 IEEE Conference on Computer Communications (INFOCOM)*. IEEE, 2015, pp. 801–809.
- [18] M. Gapeyenko, D. Moltchanov, S. Dmitriy, and R. W. Heath Jr, "Line-of-sight probability for mmwave-based uav communications in 3d urban grid deployments," *IEEE Transactions On Wireless Communications*, vol. 20, no. 10, pp. 6566–6579, 2021.
- [19] T. Kohyama and T. Hara, "Frequency distribution of tree growth rate in natural forest stands," *Annals of Botany*, vol. 64, no. 1, pp. 47–57, 1989.
- [20] J. M. Felfili, "Diameter and height distributions in a gallery forest tree community and some of its main species in central brazil over a six-year period (1985-1991)," *Brazilian Journal of Botany*, vol. 20, no. 2, pp. 155–162, 1997.
- [21] F. Mauro, R. Valbuena, J. Manzanera, and A. García-Abril, "Influence of global navigation satellite system errors in positioning inventory plots for tree-height distribution studies," *Canadian journal of forest research*, vol. 41, no. 1, pp. 11–23, 2011.
- [22] I. S. Gradshteyn and I. M. Ryzhik, *Table of Integrals, Series, and Products*. Academic press, 2014.
- [23] T. S. Rappaport, S. Sun, R. Mayzus, H. Zhao, Y. Azar, K. Wang, G. N. Wong, J. K. Schulz, M. Samimi, and F. Gutierrez, "Millimeter wave mobile communications for 5g cellular: It will work!" *IEEE Access*, vol. 1, pp. 335–349, 2013.
- [24] Y. Rahayu and M. I. Hidayat, "Design of 28/38 GHz dual-band triangular-shaped slot microstrip antenna array for 5G applications," in *International Conference on Telematics and Future Generation Networks (TAFGEN)*, 2018, pp. 93–97.